Forest Ecology and Management 432 (2019) 932–941

Contents lists available at ScienceDirect

Forest Ecology and Management

journal homepage: www.elsevier.com/locate/foreco

Change in microbial communities, soil enzyme and metabolic activity in a *Torreya grandis* plantation in response to root rot disease

Yuxing Feng[a], Yuanyuan Hu[a], Jiasheng Wu[a,*], Junhui Chen[a,b,**], Kim Yrjälä[a], Weiwu Yu[a]

[a] State Key Laboratory of Subtropical Silviculture, Zhejiang A&F University, Lin'an, Hangzhou 311300, China
[b] Zhejiang Provincial Key Laboratory of Carbon Cycling in Forest Ecosystems and Carbon Sequestration, School of Environmental and Resource Sciences, Zhejiang A&F University, Lin'an, Hangzhou 311300, China

ARTICLE INFO

Keywords:
Bacterial and fungal communities
Soil organic carbon
Microbial metabolic activity
Illumina MiSeq sequencing

ABSTRACT

Soil microorganisms have a profound influence on plant growth, but as well on plant disease. It is still not clear, however, how microbial community structures and functional activities are changing in transitions between healthy and diseased soils. We performed detailed bacterial and fungal community analysis in healthy and root-rot diseased soils of *Torreya grandis* plantation forest in the subtropical region of China. Soil enzyme activities and microbial metabolic profiling was done to find their interactions with the diseased plants and the microbial functioning. The diseased trees showed lower root biomass, total chlorophyll and N contents in leaf, but higher peroxidase activity. The soils under diseased trees had lower soil organic carbon (SOC) content, but higher pH, moisture and available N content. The microbial diversity was unchanged between the healthy and diseased soils, but the diseased soils had lower 16S rRNA and ITS gene copy numbers. Illumina MiSeq sequencing showed that the fungal rather than the bacterial community composition differed significantly ($P < 0.05$) and *Gibberella* and *Cryptococcus* were associated with the diseased trees. The activities of β-D-cellobiosidase, β-glucosidase and peroxidase and microbial carbohydrate utilization rates were typically enhanced in the diseased soils. Changes in SOC, available N and soil moisture associated to root-rot disease were key factors shaping microbial community composition and activity, and closely linked to plant biomass. Our study showed that prolonged root-rot infestation decreased tree vitality and soil microbial biomass, changed fungal community composition and soil functioning towards a faster organic C decomposition, which potentially may increase soil organic matter turnover.

1. Introduction

Torreya, a genus of conifers comprising six species within the family of Taxaceae, is mainly distributed in South China (Li et al., 2014; Zhang et al., 2017, 2019), but also in California and western Florida in the United States and some parts of Japan and Korea (Kang and Tang, 1995). Among this genus, *Torreya grandis* cv. Merrillii is an economically important nut tree species that is endemic in China. Due to their high economic value, *T. grandis* plantations have rapidly been expanded in the past three decades through converting native forests into plantations. Such expansion of *T. grandis* plantations has, however, resulted in environmental problems such as soil erosion and biodiversity loss, and creation of favorable conditions for development of soil borne disease due to improper forest management (Wang and Lu, 2017).

Root-rot is one of the main catastrophic diseases of *T. grandis*. Symptoms of the roots infected by root-rot disease are crown rot characterized by light-brown discoloration of the cambium with brownish black necrotic areas (Zhang et al., 2016). Diseased trees have shown reduced vigor and chlorosis on the foliage resulting in death of plant, which causes yield reduction and serious economic losses. The *T. grandis* root-rot has been demonstrated to be caused by *Fusarium oxysporum* species complex, a ubiquitous soil-borne pathogen comprising more than 100 host-specific strains (formae speciales) (Zhang et al., 2016; Gordon, 2017). Root-rot of *T. grandis* is more commonly observed in newly pioneered orchards of these tree crops, where the soil environments are disturbed by improper soil management making the young trees more vulnerable to disease. Though it is clear that root-rot could cause significant and negative changes in the aboveground biomass, it is unclear how soil microbial communities are changing in transitions between healthy and diseased soils.

* Corresponding author at: State Key Laboratory of Subtropical Silviculture, Zhejiang A&F University, Lin'an, Hangzhou 311300, China.
** Corresponding author at: State Key Laboratory of Subtropical Silviculture, Zhejiang A&F University, Lin'an, Hangzhou 311300, China.
E-mail addresses: wujs@zafu.edu.cn (J. Wu), junhui@zafu.edu.cn (J. Chen).

https://doi.org/10.1016/j.foreco.2018.10.028
Received 20 June 2018; Received in revised form 27 September 2018; Accepted 13 October 2018
Available online 20 October 2018
0378-1127/

Soil microorganisms are critical to soil biogeochemical processes, and their diversity and community composition play a key role in determining soil functionality (Wagg et al., 2014). Soil microbial communities are highly relevant to the suppression or outbreak of soil-borne plant diseases (Garbeva et al., 2004; Wei et al., 2015). A number of studies have suggested that the interactions between plant roots, soil microorganisms and soil properties modulate plant health through promoting or suppressing soil borne pathogens, consequently plant performance (Garbeva et al., 2004; Xu et al., 2012; Wei et al., 2015; Campos et al., 2016). Plants roots exert strong influences on both soil borne pathogens and beneficial microorganisms in the rhizosphere by producing exudates as well as secondary metabolites (Dennis et al., 2010; Wu et al., 2016). While higher soil microbial diversity was reported to be associated with lower disease incidence (Bakker et al., 2010; Brussaard et al., 2007). Under unfavorable conditions, however, the interactions between plants, soil and microorganisms may lead to the development of disease (Janvier et al., 2007). Nevertheless, the host-pathogen interactions are multifaceted under natural field conditions (Davies and Pedersen, 2008). Better knowledge of microbial community structures in root zone soils at plantations in combination with soil quality data, could facilitate the development of management strategies to improve plant health and soil fertility.

Although we know that *T. grandis* root rot is caused by the *Fusarium* pathogenic fungi, few studies have investigated the effects of root-rot disease and its induced changes in plant performance on soil microbial communities. The plant performance influenced by prolonged root-rot disease have been shown to affect the microbial community composition via alterations in soil environment (Ruotsalainen and Eskelinen, 2011). Root-rot plants also change root morphology, mineral nutrients uptake and cause leakage of organic root constituents, which leads to distinct ecological conditions of rhizosphere colonization (Yang et al., 2001; Chapon et al., 2002; Kyselkova et al., 2009). It was reported that decreases in *Picea abies* vitality and allocation of photosynthates belowground in *Heterobasidion* due to root-rot infection, could change the composition of fungal communities in the rhizosphere (Gaitnieks et al., 2016). As both beneficial microbes and pathogens are likely to interact in root-zone soils, the entire microbial community needs to be studied in diseased soils.

Furthermore, in order to explore the mechanism of the root-rot disease and to develop efficient biological control strategies, the changes in soil functionality should also be addressed. For example, infestation of violet root rot was shown to increase bacterial abundance and fluorescein diacetate hydrolysis in the root zone of an apple orchard (Shishido et al., 2008). Pathogens induced changes in soil habitats may also affect microbial metabolic functioning and soil extracellular enzyme activities, both of which are considered as sensitive indicators of disturbances and environmental stress (Marschner et al., 2003; Sinsabaugh et al., 2008). To the best of our knowledge, the soil microbes, both bacteria and fungi, have not previously been compared in detail between diseased (root rot) and healthy root zones accompanied with soil enzyme and functional metabolic profiling. Thus, the objective of this study was (1) to characterize the interactions between plant, soil and microbial community in healthy and root rot diseased *T. grandis* trees, and (2) to illustrate the difference in physiology of healthy and diseased plants.

2. Material and methods

2.1. Site information

The study site is located in a plantation of *T. grandis* cv. Merrillii in Lin'an (30°20′39″N, 119°37′26″E), Hangzhou City, Zhejiang Province, China. The region has a monsoonal subtropical climate, with mean annual precipitation of 1450 mm and temperature of 16.0 °C, respectively, and the elevation is approximately 250 m above sea level. The soil is classified as Ferrisols in the FAO soil classification system with a sandy loam texture. The studied plantation of *T. grandis* has an area of approximately 20 ha, and was converted from Moso bamboo (*Phyllostachys pubescens*) forest. *T. grandis* have been cultivated for 12 years according to local management practices. Chemical fertilizers, urea (145 kg ha^{-1}), super phosphate (100 kg ha^{-1}) and potassium chloride (45 kg ha^{-1}) were applied annually to the studied area, of which 60% was applied as basal fertilizer in late March and 40% as supplementary fertilizer followed by soil tillage in October. Plants were spaced at 3 m × 3 m, with an average tree height of approximately 2.9 m. The incidence of root-rot disease of *T. grandis* in this plantation is about 20% based on the observation of typical symptoms described by Zhang et al. (2016). The diseased trees in this site have been infested for more than 4 years with *Fusarium oxysporum* species complex, a casual agent of root rot.

2.2. Sample collection

Within the *T. grandis* plantation, three plots with an area of 20 m × 20 m at a 10 m interval distance were selected. The plots have similar soil type with consistent altitude and management practices. In each plot, three or four root-rot diseased but still living trees of *T. grandis* (caused by *Fusarium oxysporum* species complex) were randomly selected in early May 2017, which all exhibited the same symptoms of root-rot disease identical to that observed by Zhang et al. (2016). Three or four healthy trees were randomly selected as control. In total, 10 healthy or diseased trees were selected. From each tree, the third or fourth fully expanded and exposed young leaves were sampled for analysis of physiological parameters. Excised leaflets were collected in plastic bags and immediately transported to the laboratory after sampling.

Ten soil cores at depth of 0–20 cm with 7 cm diameter, were randomly collected around the tree trunk within a diameter of 1 m after removing the litter layer. The soil cores were thoroughly mixed to make a single composite sample. The composite samples were then transferred to sterile plastic bags, sealed and placed on ice to be transported to the laboratory immediately after sampling. The soil samples were thoroughly homogenized and sieved with a 2 mm mesh, and plant materials and gravels, if any, were removed. Aliquots of fresh soil samples were stored at 4 °C and −70 °C for biological analysis and DNA extraction, respectively, and air-dried samples were passed through a 0.25 mm sieve for chemical analysis.

2.3. Analysis of plant physiological parameters

Root biomass was measured during soil homogenization processing when roots were picked out from the sieve by hand, washed in water, oven dried at 65 °C and weighed. The aboveground biomass was estimated based on the data of tree height, diameter at breast height and crown length according to the method described by Qian et al. (2013). Foliar water content (%) was determined by mass difference after drying at 65 °C until constant weight. The foliar N concentrations were determined via flash combustion using a Carlo-Erba EA 1108 analyser (Italy). Total chlorophylls contents were estimated according to the protocol described by Harmut and Lichtenthaler (1987) and expressed in mg g^{-1} fresh weight (FW). The soluble protein content was measured according to Bradford (1976). The relative electrolyte conductivity of leaf was used to estimate membrane permeability according to the protocol described by Nayyar (2003). Foliar peroxidase (POD) activity was measured with guaiacol at 470 nm according to Fu and Huang (2001).

2.4. Analysis of soil physicochemical properties

Soil pH was determined with a pH meter using a soil-to-water ratio of 1:2.5. Soil moisture content (%) was determined by mass difference after drying at 105 °C until constant weight. Soil bulk density of the

topsoil was measured using 100-cm^3 cylinders. Soil organic carbon (SOC) and total nitrogen (TN) contents were determined via wet digestion using $K_2Cr_2O_7$ oxidation and the Kjeldahl method according to Lu (2000), respectively. Soil available N was assayed by using the alkaline hydrolysis method following the protocol described by Lu (2000). Soil available phosphorus (P) (Bray 1-P, 0.03 M NH_4F + 0.025 M HCl extractable) and available potassium (K) was determined by the flame photometric method (extracted by 1 M NH_4OAc) according to the procedures described by Soil Science Society of China (1999).

2.5. Soil DNA extraction and real-time PCR

Soil DNA was extracted with the E.Z.N.A.® Soil DNA Kit (D4015, Omega, Inc., USA) according to the manufacturer's instructions. Bacterial 16S rRNA and fungal internal transcribed spacer (ITS) gene abundances were determined using primer sets 338F/518R and 5.8s/ITS1F, respectively (Fierer et al., 2005). The quantitative polymerase chain reactions (PCR) were carried out in an iCycler IQ5 Thermocycler (Bio-Rad Laboratories Inc., Hercules, CA, USA) based on fluorometric monitoring with SYBR Green 1 dye. The PCR mixture contained 0.2 mg ml^{-1} BSA, 1–10 ng DNA, 0.2 μM of each primer and 12.5 μL of SYBR premix EX Taq™ (Takara Shuzo, Shiga, Japan). The PCR conditions were as follows: 95 °C for 3 min; 35 cycles of 30 s at 95 °C, 30 s at 55 °C and 40 s at 72 °C, and finally 10 min at 72 °C. Products specificity of PCR was checked by melting curve analysis and visualization by agarose gel electrophoresis. Copy numbers of the genes in soil samples were determined using a standard curve generated using purified template plasmid DNA as described in our previous study (Chen et al., 2016).

2.6. Illumina MiSeq sequencing and data processing

Bacterial and fungal community compositions in each soil were determined by Illumina Miseq sequencing. In brief, the primer pair 515F (5′-GTGYCAGCMGCCGCGGTAA-3′) and 806R (5′-GGACTACHVGGGTWTCTAAT-3′) with unique 12nt barcode was used to amplify the V4 region of bacterial 16S rRNA gene. The primer pair ITS7 (5′-GTGARTCATCGAATCTTTG -3′) and ITS4 (5′-TCCTCCGCTTATTGATATGC-3′) was used to amplify fungal internal transcribed spacer (ITS) 2 region. PCR reaction mixture contained 10 ng of template DNA, 12.5 μL PCR Premix, 2.5 μL of each primer, and PCR-grade water in a final volume of 25 μL. The PCR amplification program included an initial denaturation at 94 °C for 3 min, followed by 30 cycles of 94 °C for 40 s, 50 °C for 60 s, and 72 °C for 60 s, and a final extension at 72 °C for 10 min. Three PCR reactions were conducted for each sample, and they were combined after PCR amplification. The PCR products were confirmed with 2% agarose gel electrophoresis, purified by AMPure XT beads (Beckman Coulter Genomics, Danvers, MA, USA) and quantified by Qubit (Invitrogen, USA). All samples were pooled together with equal molar amount from each sample. The pooled samples were paired-end sequenced (2 × 250) on an Illumina MiSeq platform (Illumina, San Diego, CA, USA) according to the standard protocols. The obtained raw reads were deposited into the NCBI Sequence Read Archive (SRA) database under the accession number of SRP140593.

Processing of the raw sequences was performed using the Quantitative Insights into Microbial Ecology (QIIME) pipeline (Caporaso et al., 2010). Paired-end reads were assigned to samples based on their unique barcode and were merged using FLASH. Reads with average quality score lower than 20, ambiguous bases and improper primers were discarded before clustering. The resultant high-quality sequences were clustered into operational taxonomic units (OTUs) at 97% similarity using UPARSE algorithm (Edgar 2013). Chimeras were checked and eliminated during clustering using U-Chime (Edgar et al., 2011). Representative sequences were chosen for individual OTU, classified by Ribosomal Database Project (RDP) Classifier. To correct for sampling effect, subsets of 14657 and 8898 sequences per sample were randomly selected for down-stream analyses for bacteria and fungi, respectively.

2.7. Physiological profiling of microbial communities

In order to elucidate the changes of microbial substrate-use patterns induced by root-rot disease, the community-level physiological profiles (CLPP) using Biolog-ECO plates was applied according to the procedure by Girvan et al. (2003). In brief, 10 g of fresh soil were shaken with 100 ml sterile water, diluted by a factor of 1000, inoculated (125-μl aliquot) into microplate well and incubated at 25 °C in the dark. Color development in the wells was measured at 590 nm with an automated plate reader (VMAX, Molecular Devices, Crawley, UK) at 24-h intervals over a 168-h incubation period.

Samples for statistical analyses were selected using the average well color development (AWCD) method at time points of 72 h. Differences in microbial metabolic potential among samples are presented using non-metric multidimensional scaling (NMDS) and tests of Analysis of Similarity (ANOSIM) (Clarke and Green 1988), and the *r* values associated to the NMDS were calculated using ANOSIM based on 999 permutations. In order to determine maximal utilization rates, the Biolog Ecoplates substrates were divided into six functional groups (carbohydrates, amino acids, carboxylic acids, amines/amides, polymers and phenolic compounds) as described previously (Choi and Dobbs, 1999) and maximum utilization rates for each of the functional groups were calculated.

2.8. Measurement of soil enzyme activity

Twelve soil enzymes involved in C (peroxidase, β-xylosidase, α-glucosidase, β-D-cellobiosidase, β-glucosidase, invertase), N (urease, chitinase, leucine aminopeptidase, N-acetyl-β-glucosaminidase), P (phosphatase) and S (arylsulfatase) cycling were selected for analysis. Among them, seven enzymes including β-xylosidase, β-D-cellobiosidase, α-glucosidase, β-glucosidase, leucine aminopeptidase, N-acetyl-β-glucosaminidase and phosphatase were analyzed according to the standard fluorescence enzyme protocol described in Bell et al. (2013). This protocol measures yields of the fluorescent cleavage products MUB (4-methylumbelliferyl) or MUC (4-methylcoumarin) via a microplate fluorometer (Synergy™ H1, Biotek) at 365 nm excitation and 450 nm emission wavelengths. Invertase activity was assayed by determination of glucose released from a sucrose solution (8%) as a substrate after incubation at 37 °C for 24 h. Urease activity was determined using urea as the substrate as described by Lu (2000). The peroxidase was measured spectrophotometrically in the clear 96-well microplate using the substrate of L-3, 4-dihydroxyphenylalanine (L-DOPA). Arylsulfatase and chitinase activities were measured using a method in which enzyme activity releases p-nitrophenol (pNP) from added substrates and levels of pNP are determined colorimetrically (Dick et al., 2013; Olander and Vitousek, 2000). Levels of pNP were measured on a Hitachi 150–20 spectrophotometer at 410 nm.

2.9. Statistical analysis

Statistical calculations were performed with the SPSS 18.0 package for Windows. Data was expressed as means ± standard deviations. Independent sample *t*-test was performed to observe the statistically significant difference for the means of healthy and diseased samples at the 95% Confidence Interval (CI). Before performing *t*-test, the normality and homogeneity of distribution of the variance were tested, and the data were log-transformed if the assumption of homogeneity was violated. The relationships between plant physiological parameters, soil characteristics and biological variables were tested using the Pearson correlation. An OTU-based analysis was performed to calculate the richness and diversity index of samples including Chao1, Shannon

diversity and Simpson index with a cutoff of 3% dissimilarity. Principal coordinates analysis (PCoA) was used to analyze the differences in microbial community composition among samples based on the Bray-Curtis distance matrix. Significance of differences of the microbial community composition between healthy and diseased plants was analysed with analysis of similarity (ANOSIM, Clarke, 1993), Adonis (permutational multivariate analysis of variance, Clarke and Warwick, 2001) multi-response permutation procedures (MRPP) were carried out based on Bray-Curtis distances by using VEGAN package in R. BioEnv and Canonical correspondence analysis (CCA) was performed to determine the main environmental factors (soil moisture, pH, SOC and available N contents, root biomass) affecting the microbial community composition using the 'vegan' package for R (v2.15.3). To determine the relative contribution of root rot disease, soil characteristics and root biomass to the composition of the microbial community, a variance partitioning analysis (VPA) was performed, which seeks to partition the total variance of the dependent variable into various portions. The significance of these environmental variables was tested with a permutation test based on 999 permutations.

3. Results

3.1. Plant physiological characteristics

The mean tree height, aboveground biomass, root biomass, physiological parameters of leaves including the water content, total chlorophyll and N contents were significantly ($P < 0.05$) lower in diseased *T. grandis* than those of healthy trees (Table 1). The activities of foliar peroxidase were, however, significantly ($P < 0.05$) higher in the diseased trees. There were no differences in relative electrolyte conductivity and soluble protein content between diseased and healthy trees.

3.2. Soil physico-chemical properties

The soil pH, moisture and available N contents were significantly ($P < 0.05$) higher by 11%, 31% and 16%, respectively, in the soils of diseased trees compared to those of the healthy trees (Table 2). In contrast, the SOC concentration was much lower in soil of the diseased plants. Other soil properties including bulk density, TN, available P, available K contents were not changed by root rot disease.

3.3. Bacterial and fungal community abundance and composition

The copy numbers of bacterial 16S rRNA and fungal ITS gene were significantly lower by 52.1% and 70.0% ($P < 0.05$) in the soils of diseased *T. grandis* compared to that of the soils from healthy trees (Table 3). The OTU numbers, Chao1, the Shannon and Simpson indices of both the bacterial and fungal communities did not differ between the healthy and diseased trees. The PCoA results showed that the bacterial communities from the diseased and healthy trees did not separate in the ordination, but the fungal communities of diseased and healthy soils displayed some separation (Fig. 1). ANOSIM, MRPP and Adonis analysis of communities confirmed significant changes in the overall fungal community composition, but not in the bacterial community composition (Table S1).

Proteobacteria, Acidobacteria and Actinobacteria were the dominant bacterial phyla in the studied soils (Fig. 2). Proteobacterial abundance was significantly 19% lower ($P = 0.02$) in the diseased soils. There were no significant differences in the relative abundances of the rest of the phyla between the diseased and healthy soils. Ascomycota and Basidiomycota were the dominating fungal phyla. The relative abundance of Zygomycota was 135% higher ($P < 0.01$) in the diseased soils. At the genus level, the most abundant bacterial genera did not differ between the diseased and healthy soils. The relative abundances of *Gibberella*, *Cryptococcus*, *Didymella*, *Mortierella* genera and *Agaricales*_unclassified genera were significantly higher by 90.2%, 124.3%, 34.7%, 114.6% and 824.0%, respectively, in the diseased soil. According to LefSe analysis, these are the potentially key genera contributing to the structural segregation of healthy and root-rot *T. grandis* (Fig. 3).

3.4. Soil enzyme activities and microbial metabolic potential

The activities of peroxidase, β-D-cellobiosidase and β-glucosidase were significantly ($P < 0.05$) higher by 24.9%, 67.8% and 53.1%, respectively, in diseased soils than in the healthy soils (Table 4). The phosphatase activity was lower by 16%, whereas the arylsulfatase activity was higher by 17% in the diseased soils. The utilization rates of carbohydrates by microbial communities were significantly ($P < 0.01$) higher in root-rot diseased soils (Fig. 4). Though statistically not significant, the utilization rates of carboxylic acids tended to be higher, but that of the phenolic compounds decreased in the diseased soils. No differences in utilization rates of other carbon sources could be found. A significant (ANOSIM's $r = 0.254$, $P = 0.003$) difference was also found between diseased and healthy samples as indicated in the NMDS ordination (stress = 0.12).

3.5. Linkage between plant performance and soil properties

The aboveground biomass, tree height, root biomass, foliar water and N contents were significantly ($P < 0.05$) and negatively correlated with soil moisture, but positively correlated with SOC (Table S2). The CCA ordination plots showed that the bacterial community changes corresponded significantly with available N ($R^2 = 0.834$, $P = 0.001$) and SOC contents ($R^2 = 0.500$, $P = 0.012$) and root biomass ($R^2 = 0.597$, $P = 0.002$) (Fig. 5, Table S3). The fungal communities varied significantly only with soil moisture ($R^2 = 0.671$, $P = 0.004$) (Table S4). VPA showed that root-rot disease, root biomass and soil properties (SOC, pH, available N and moisture) totally explained 42.3% and 35.3% of the observed variation of bacterial and fungal communities, leaving 57.7% and 64.7% of the variation unexplained, respectively (Fig. 6). The soil properties explained the largest portion of the observed variations for both bacterial (26.0%) and fungal (20.9%) communities, followed by root biomass. The interactions between these variables accounted for a small part of the observed variations.

RDA indicated significant (ANOSIM's $r = 0.319$, $P = 0.002$) differences in enzyme activities between the diseased and healthy soils

Table 1
The plant growth and physiological parameters (mean ± SD, n = 10) of diseased and healthy *T. grandis*.

	Tree height (m)	Aboveground biomass (kg)	Root biomass (g m^{-2})	Total chlorophyll content (mg g^{-1} FW)	Foliar water content (%)	Foliar N content (mg g^{-1})	Soluble protein content (mg g^{-1} FW)	Foliar peroxidase (U g^{-1} FW min^{-1})	Relative electrolyte conductivity (%)
Healthy	3.23 ± 0.46	4.58 ± 1.65	336.32 ± 110.26	1.04 ± 0.20	65.19 ± 2.75	21.44 ± 2.41	24.39 ± 2.48	11357.56 ± 2055.63	88.61 ± 5.26
Diseased	1.96 ± 0.28	1.77 ± 0.76	149.43 ± 49.06	0.25 ± 0.18	62.40 ± 2.01	15.13 ± 1.73	23.38 ± 2.02	13895.26 ± 2168.38	89.43 ± 6.01
Sig.	***	***	***	***	*	***	NS	*	NS

Sig. significance. *** $P < 0.001$, ** $P < 0.01$, * $P < 0.05$, NS $P > 0.05$.

Table 2
The soil physico-chemical properties (mean ± SD, n = 10) of diseased and healthy *T. grandis* soil.

	pH (H_2O)	Moisture (%)	Bulk density (g cm^{-3})	SOC (g kg^{-1})	TN (g kg^{-1})	Available N (mg kg^{-1})	Available P (mg kg^{-1})	Available K (mg kg^{-1})
Healthy	4.86 ± 0.11	14.32 ± 1.62	1.02 ± 0.13	28.35 ± 5.33	2.48 ± 0.30	108.68 ± 8.82	193.67 ± 11.24	38.09 ± 8.50
Diseased	5.44 ± 0.75	20.64 ± 5.07	1.01 ± 0.08	23.80 ± 2.84	2.40 ± 0.36	128.93 ± 22.45	182.97 ± 21.24	33.71 ± 9.17
Sig.	*	**	NS	*	NS	*	NS	NS

SOC, soil organic carbon; TN, total nitrogen content; Sig. significance ** $P < 0.01$, * $P < 0.05$, NS $P > 0.05$.

(Fig. 7). The enzyme activities of diseased soil samples were clearly separated from those of healthy along the first axis in the ordination space. The enzyme activities of diseased soils had significant correlations with the fungal community composition (indicated by PCoA 1) ($R^2 = 0.300$, $P = 0.047$), soil moisture ($R^2 = 0.460$, $P = 0.008$) and microbial carbon utilization rates ($R^2 = 0.323$, $P = 0.026$), whereas the healthy soils were significantly correlated with root biomass ($R^2 = 0.487$, $P = 0.005$) and fungal abundance ($R^2 = 0.306$, $P = 0.044$). Soil moisture and microbial carbon utilization rates were positively correlated with β-D-cellobiosidase (CB) and β-glucosidase (BG) activities, and explained 14%, 14% and 13% of the variance, respectively.

4. Discussion

The role of pathogens in the *T. grandis* root rot complex is well studied, but not much is known about the role of the entire microbial community in diseased soils and their effects on soil functional activity. The big question in studies of plant performance and plant disease caused by pathogenic fungi is the interaction between above ground and below ground organismal processes. In our study the root rot disease altered the biological activity of soil shown by changed fungal community, lower microbial biomass but significantly higher utilization rates of carbohydrates by microbial communities.

The combined analysis of microbial communities, their catabolic activity, soil characteristics and plant parameters allows acquiring important knowledge of *Fusarium oxysporum* generated root rot in tree species. In our study, we primarily detect the consequences of the *Fusarium* induced changes in the plant performance, but also the diseased woody plant's interaction with the belowground soil and there with the bacterial and fungal communities. Our study suggests that fungal rather than bacterial community composition was altered in the soils where diseased plants were growing and microbial abundance was reduced, and at the same time plant performance was reduced with lower plant biomass and total N and chlorophyll content. Changes in soil attributes, such as SOC, available N and soil moisture, explained the reduction in microbial abundance both bacterial and fungal, and were key factors shaping the community composition. The fungal taxa *Gibberella*, *Cryptococcus*, *Mortierella* and *Lectera* were identified to be associated with root-rot *T. grandis*.

The root-rot diseased *T. grandis* not only showed lower aboveground and root biomass, but also decreased total chlorophyll and N contents. The observed decrease in root biomass in the diseased trees was inconsistent with Gaitnieks et al. (2016), who observed that root-rot had little effect on fine root morphology despite the significantly higher defoliation in root-rot infected *Picea abies* stands. As the plantation of healthy and diseased *T. grandis* had similar soil properties, local climate conditions and management practice, our results suggested a reduction in tree vitality and plant growth after long period of root-rot infection. Foliar peroxidase (POD) is an enzymatic antioxidant, evolved as an effective scavenging system to alleviate the harmful effects of reactive oxygen species in plant when subjected to physiological stress (Li et al., 2014). Although it is suggested that young *T. grandis* trees could still survive for a few years until death after infection with root-rot disease (Sun and Yang, 2003), the dramatically higher foliar antioxidant POD activity of diseased plants supports the notion of long disease period causing biotic stress induced by root-rot disease.

Changes in plant performance may affect soil nutrient dynamics and microbial community compositions through influencing organic matter input, which in turn could have feedback on plant health. Our results showed that the soils of diseased plants were associated with a lower SOC concentration but a higher pH, probably due to lower organic matter input and accelerated SOC depletion. SOC concentration is normally balanced by multiple input and loss of pathways of soil C dynamics (Kennedy, 1999). The significant and positive correlations between aboveground and root biomass and SOC contents in this study suggested that lower aboveground biomass of diseased trees may have reduced the litter input, products of photosynthesis or root exudates into soils, contributing to the lower SOC accumulation during the time of prolonged disease. Further, it is possible that root-rot disease accelerated SOC decomposition through increasing microbial community activity in the root zone soils, which is supported by the higher enzyme activities involving C cycling and microbial carbon use rate observed in current study (Fig. 4 and Table 4). As soil organic matter is an important indicator of soil health and quality (Garbeva et al., 2004), the depletion of SOC in the diseased soil may in turn further decrease plant pathogen resistance or suppression (Janvier et al., 2007). Being in line with the observation by Gaitnieks et al. (2016), the higher pH values in the diseased soils might be associated with the lower litter input or root exudates into soils. In addition, we found that the foliar water content was negatively correlated with soil moisture, suggesting that decreased health status of leaf reduced transpiration and resulted in higher water accumulation in soil. Our results support previous observation that higher incidence of *T. grandis* root-rot disease was usually associated with higher soil moisture (Sun and Yang, 2003), which may create more favorable conditions for the incidence and transmission of pathogens. Similarly, the higher available N contents in the diseased soils may be ascribed to lower N uptake of plants.

It has been suggested that lower microbial diversity in the rhizosphere soils may lead to higher occurrence of soil borne disease (Bailey

Table 3
The gene abundance and α-diversity indices (mean ± SD, n = 10) of soil bacterial and fungal communities in the soils of healthy and diseased *T. grandis*.

		Gene abundance (× 10^8 copies g^{-1})	OTUs	Chao1	Shannon	Simpson
Bacterial 16S rRNA gene	Healthy	666.08 ± 479.34	2809.8 ± 76.86	4012.91 ± 145.21	9.99 ± 0.26	0.997 ± 0.002
	Diseased	319.06 ± 51.49	2787.8 ± 285.33	4118.80 ± 336.90	9.81 ± 0.49	0.995 ± 0.004
	Sig.	*	NS	NS	NS	NS
Fungal ITS gene	Healthy	6.05 ± 6.17	314.60 ± 55.97	372.14 ± 50.81	5.64 ± 1.38	0.900 ± 0.163
	Diseased	1.81 ± 1.01	317.90 ± 23.12	365.13 ± 39.22	6.41 ± 0.31	0.971 ± 0.126
	Sig.	*	NS	NS	NS	NS

Sig. significance, * $P < 0.05$, NS $P > 0.05$.

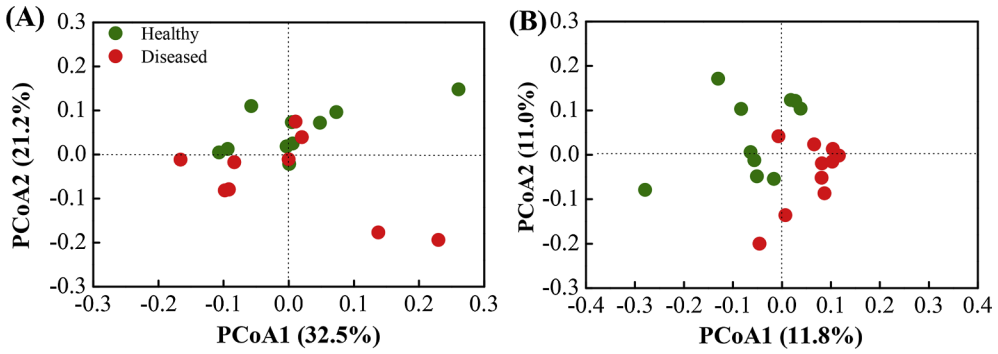

Fig. 1. Principal coordinates analysis (PCoA) ordinations based on Bray-Curtis distances showing the changes in bacterial (A) and fungal (B) community compositions in the soils of healthy and diseased *T. grandis*.

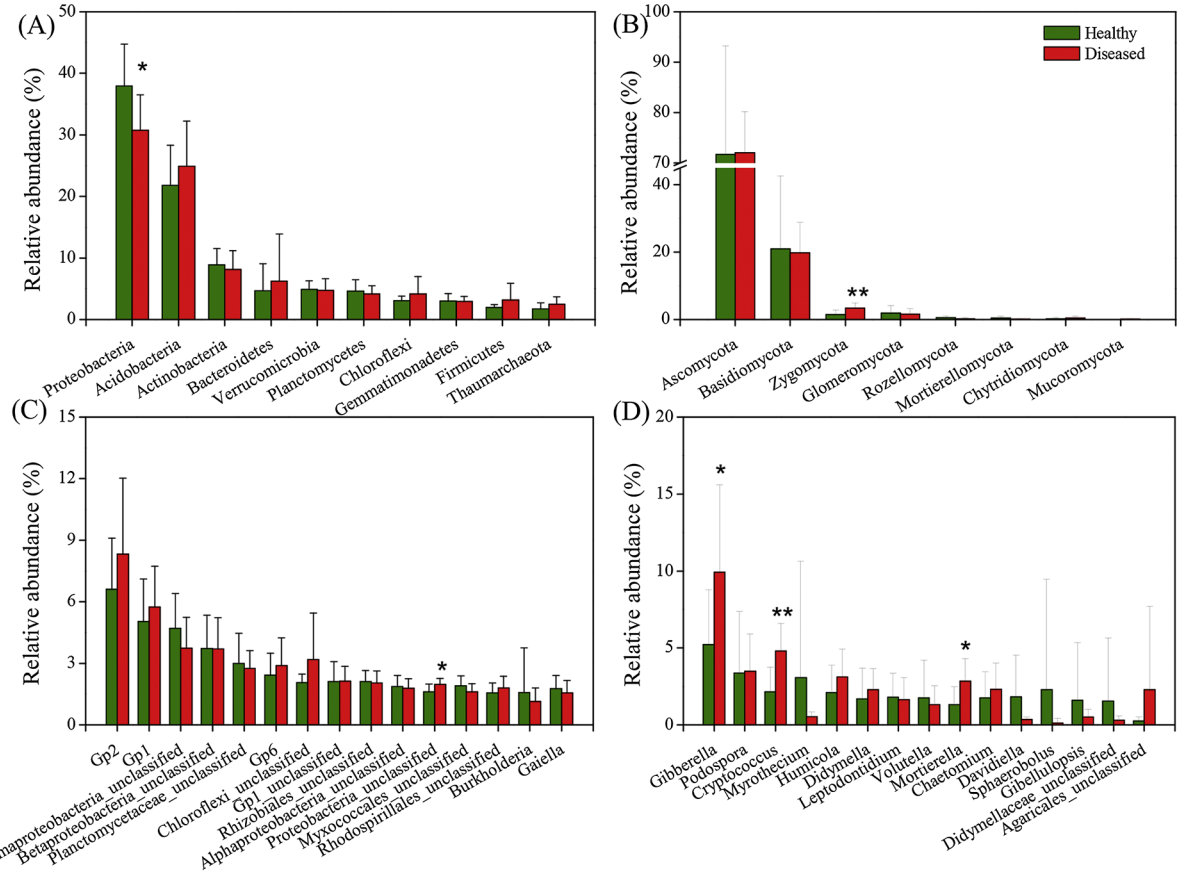

Fig. 2. The relative abundance of the dominant bacterial phyla (A), fungal phyla (B), bacterial genus (C) and fungal genus (D) in soils of healthy and diseased *T. grandis*. The asterisks over the error bars indicate a significant difference between healthy and diseased plants based on a *t*-test at $P < 0.01$ (**) or $P < 0.05$ (*).

and Lazarovits, 2003; Wu et al., 2015). Microbial diversity is of great importance to resilience towards disturbance (Tilman et al., 2006). Wu et al. (2015) found that microbial communities in rhizosphere soils of diseased *P. notoginseng* showed a decrease in alpha diversity in comparison with those of healthy plants. With detailed microbial analysis, we observed no significant differences neither in bacterial nor in fungal community diversity in the soil between healthy and diseased plants (Table 3). This could be explained by the fact that some key or functional species rather than the overall microbial community diversity are more important to disease control (Griffiths et al., 2001). Our study confirmed the finding by Donegan et al. (1996) that microbial diversity was not effective to independently predict soil health due to their functional redundancy. Soil pH has been accepted as a primary abiotic factor for bacterial growth and phylogenetic diversity (Fierer and Jackson, 2006). We found that although the pH was much higher in diseased than healthy soils, the bacterial diversity index was unchanged, suggesting a constrained community in the diseased soil showing a prolonged diseased state of the soil. The concomitant unchanged bacterial community diversity and structure in the soils subjected to root-rot may indicate a high robustness of microbial community structure to both abiotic (such as soil acidification, SOC depletion) and biotic (such as allelopathy) changes induced by disease. We found, however, that both the bacterial and fungal abundance were strikingly lower in the soils of diseased trees, which was in disagreement with the findings by Wu et al. (2016) who revealed that the abundances of bacteria and fungi in the rhizosphere soil of diseased *Panax notoginseng* plants were significantly higher than those of healthy plants. Soil microbial biomass is closely linked to nutrient availability, such as SOC concentrations (Burton et al., 2010), and the lower SOC contents in the soils of diseased trees in our study may partly explain

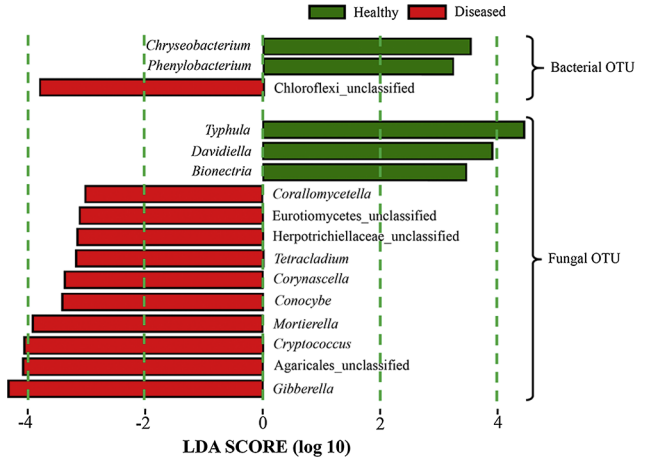

Fig. 3. Linear discriminant analysis (LDA) coupled with effect size measurements to identify the differential genera in soils of healthy versus diseased *T. grandis* (defined as LDA scores > 2.5). Healthy plants-enriched genera are indicated with a positive LDA score (green), and genera enriched in root-rot diseased plants has a negative score (red). (For interpretation of the references to color in this figure legend, the reader is referred to the web version of this article.)

such decrease in biomass. It is probable that the small aboveground biomass and lower chlorophyll contents in the leaves of diseased *T. grandis* may decrease the input of organic compounds into soil, which potentially reduced the soil microbial biomass. These results indicate that root-rot may induce physiological stress for tree growth and create a poor soil habitat for microbial growth.

Clear changes in soil microbial community composition induced by root-rot disease has been reported frequently for other crops such as tobacco (Kyselkova et al., 2009), pea (Xu et al., 2012), peanut (Li et al., 2014), Sanqi (*Panax notoginseng*) and apple (Shishido et al., 2008). The current study showed that the fungal rather than bacterial community composition in the diseased soils differed from that of the healthy soils as indicated by PCoA (Fig. 2), suggesting that the entire fungal community is more sensitive to root-rot disease and changes in soil characteristics. The greater changes in fungal community composition than that of bacteria was in accordance with the previous findings (Durner et al., 1997; Creelman and Mullet, 1997). To identify taxa indicative of soil disease status, we compared the microbial community compositions in the soils at phylum and genus level. Being in line with the PCoA results, the majority of the relative abundances of phyla of bacteria and fungi differed little between the diseased and healthy soils (Fig. 2). Indeed, only a few taxa, in particular for fungal community, were significantly changed in soils of diseased trees. The genera of *Gibberella*, *Cryptococcus*, *Didymella* and *Mortierella* contributed greatly to the changes in fungal community composition (Fig. 3), most of which are commonly encountered as the major virulence factor in plant disease (Benny and Blackwell, 2004). The higher abundance of these fungal

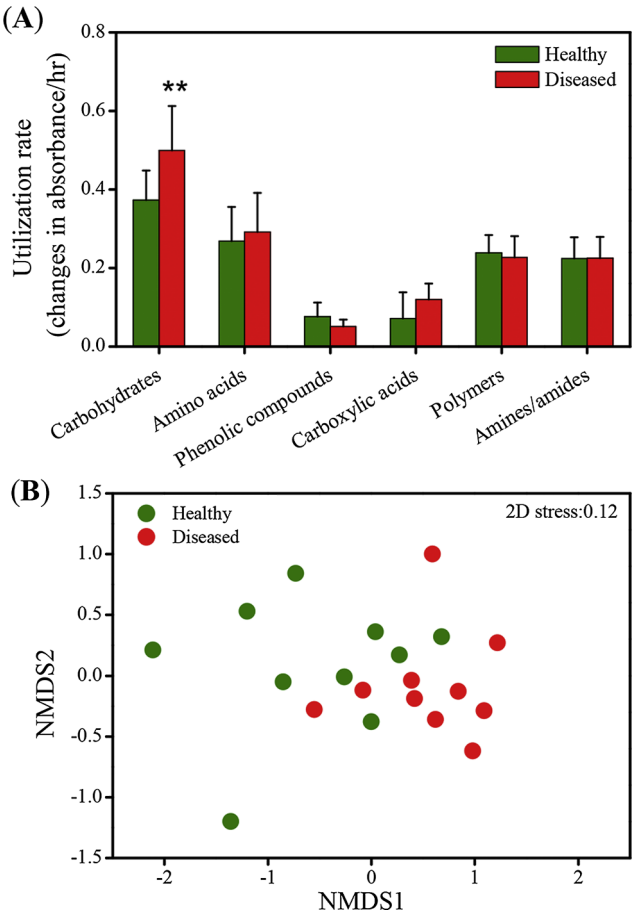

Fig. 4. (A) Carbon source utilization rates of soil microbial communities of healthy and diseased *T. grandis* based on specific carbon families. Bars present ± SD. Asterisks over the error bars indicate a significant difference between healthy and diseased plants based on a *t*-test at $P < 0.01$ (**). (B) NMDS ordination plot of the carbon source utilization patterns of soil microbial communities of healthy and diseased *T. grandis* obtained with Biolog Ecoplates.

genera in diseased soils suggests a potential role in root rot infestation. A number of studies have demonstrated that shifts in microbial community composition are closely related to changes in soil environments (Rousk et al., 2010; Brockett et al., 2012; Chen et al., 2017). Variation partitioning analysis (VPA) in current study confirmed that changes in soil properties contributed more to the shifts in both bacterial and fungal community compositions than rootbiomass and root-rot disease. Soil property changes associated with root rot disease played a key role in shaping microbial community composition. Soil available N and SOC contents rather than pH were significantly correlated to the shifts in bacterial community compositions (Fig. 5), which indicated that bacterial communities are more sensitive to nutrient availability. Previous

Table 4
The enzyme activities (nmol product g^{-1} dry soil h^{-1}, mean ± SD, n = 10) in soils of healthy and diseased *T. grandis*.

	Peroxidase	Invertase	β-Xylosidase	β-D-Cellobiosidase	β-Glucosidase	α-Glucosidase
Healthy	1029.89 ± 137.33	5096.32 ± 548.87	5.23 ± 1.03	4.74 ± 1.46	21.38 ± 4.47	4.20 ± 0.93
Diseased	1286.34 ± 184.11	6191.06 ± 1950.61	5.94 ± 2.45	7.96 ± 2.33	32.74 ± 8.46	4.58 ± 1.13
Sig.	**	NS	NS	**	**	NS

	Urease	Chitinase	Leucine aminopeptidase	N-acetyl-β-glucosaminidase	Phosphatase	Arylsulfatase
Healthy	1941.12 ± 366.13	200.08 ± 11.01	17.62 ± 2.98	11.03 ± 2.39	124.35 ± 20.84	1256.04 ± 272.79
Diseased	2043.35 ± 682.07	199.24 ± 7.88	18.07 ± 2.73	13.41 ± 5.37	104.36 ± 17.17	1593.85 ± 294.55
Sig.	NS	NS	NS	NS	*	*

Sig. significance, ** $P < 0.01$, * $P < 0.05$, NS $P > 0.05$.

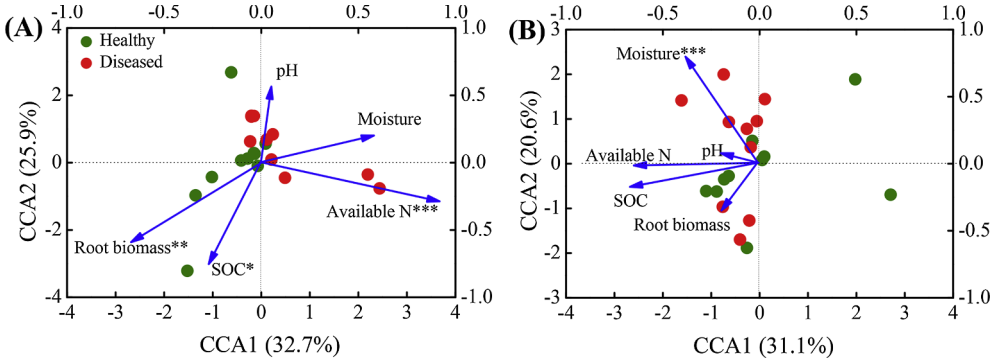

Fig. 5. Canonical correspondence analysis (CCA) of bacterial (A) and fungal community compositions (B) and environmental variables for individual samples from healthy and diseased *T. grandis*. Arrows represent environmental variables that correlated with the microbial community composition. SOC, soil organic carbon; Moisture, soil moisture. $^{*}P < 0.05$, $^{**}P < 0.01$, $^{***}P < 0.001$ indicate significant correlations.

studies suggest that fungal community composition can be affected by SOC content and C/N ratio since fungi are main decomposers of soil organic matter, while organic matter with a high C/N ratio has a strong effect on fungal composition (Thiet et al., 2006; Qin et al., 2014; Chen et al., 2018). We found that only soil moisture was significantly correlated to the shifts in fungal community composition, which agrees with the finding by Brockett et al. (2012) who demonstrated that soil moisture was the major factor influencing microbial community structure and enzyme activities across forest soils.

The Biolog assays can reveal metabolic differences between the soil microbial communities, although it usually detects only a few metabolically active and culturable heterotrophs (Nannipieri et al., 2003). Our study showed that the microbial metabolic potential of C sources was enhanced in the soils of root-rot diseased *T. grandis*. This result suggests an enhanced functional capacity of diseased soils probably due to the selection of specific microorganisms that canutilize more carbohydrates and carboxylic acids. The observed increase in metabolic potential of carbohydrates in the diseased soils in this study may also be linked to the increased abundances of root zone-associated microbial taxa, such as Chloroflexi, *Didymella* and *Mortierella*, which have been known to degrade carbohydrates compounds (Chen et al., 2016). This is possible since root necrosis induced by root-rot disease is known to cause leakage of organic root constituents, such as sugars, organic acids, and amino acids, into the soil, which may selectively lead to enhancement of associated microbial taxa (Yang et al., 2001; Chapon et al., 2002; Doornbos et al., 2012).

From a functional perspective, soil enzymes activities are the primary biological mechanism of nutrient cycling and organic matter decomposition (Nannipieri et al., 2012). Being in accordance with the results of microbial metabolic profiling, the enzyme activities determined in our study especially those involved in C cycling (i.e., β-D-cellobiosidase, β-glucosidase and peroxidase) were significantly higher in soils of the diseased plants. This is a noteworthy finding, and suggests an improved mineralization and turnover of organic C compounds and a selected effect of root rot disease on these enzyme activities.

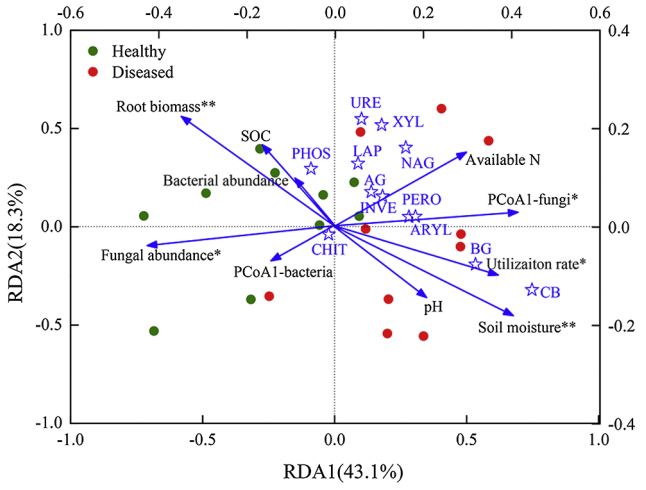

Fig. 7. Redundancy analysis (RDA) of soil enzyme activities constrained by soil physico-chemical and biological properties under healthy and diseased *T. grandis*. SOC, soil organic carbon; Utilization rate, microbial carbon utilization rates. $^{*}P < 0.05$ and $^{**}P < 0.01$ indicate significant correlations. The stars in blue indicate the enzyme activities. AG, α-glucosidase; BG, β-glucosidase; CB, β-D-cellobiosidase; XYL, β-xylosidase; NAG, N-acetyl-β-glucosaminidase; LAP, Leucine aminopeptidase; PHOS, Phosphatase; PERO, Peroxidase; URE, Urease; CHIT, Chitinase; IVER, Invertase; ARYL, Arylsulfatase. (For interpretation of the references to color in this figure legend, the reader is referred to the web version of this article.)

Hydrolases, such as cellobiosidase and β-glucosidase, are of great importance in hydrolysis of organic molecules for the release of soil nutrients for plants (Nannipieri et al., 2012). The increases in activities of these soil enzymes can accelerate soil organic matter turnover and may contribute to the lower SOC concentrations in the soils of diseased trees. We further found that the β-D-cellobiosidase and β-glucosidase were positively correlated with microbial metabolic potential as well as soil

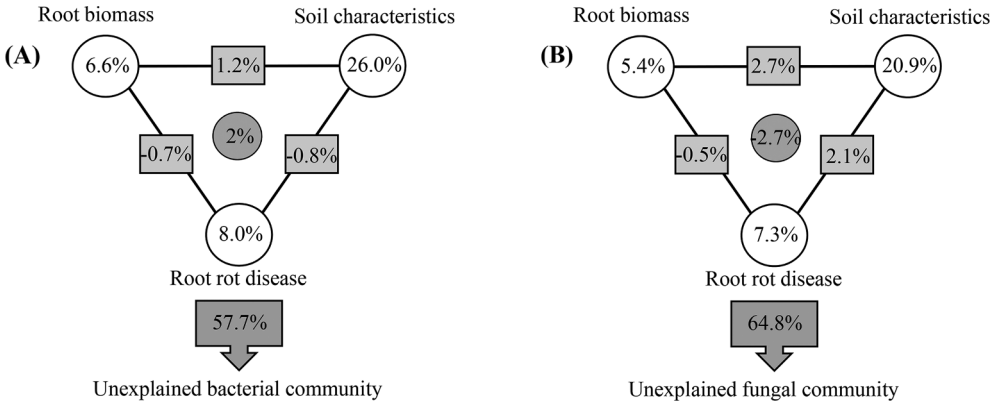

Fig. 6. Variation partitioning analysis (VPA) was used to determine the effects of soil characteristics, root biomass and root-rot disease and interactions between these parameters on the structure of the bacterial (A) and fungal (B) community. Circles on the edges of the triangle show the percentage of variation explained by each set of factors alone. The percentage of variation explained by interactions between two or three variable factors is designated by rectangles on the sides or a circle in the middle of the triangle. The unexplained variation is depicted as a rectangle at the bottom.

moisture, but negatively correlated with SOC and root biomass (Fig. 7). Such positive correlations confirmed that changes in microbial metabolic capacity was connected to regulation of soil enzyme activities (Wittmann et al., 2004). Because soil enzymes mainly originate from soil microorganisms, changes in microbial metabolic activity would potentially affect enzyme activities (Nannipieri et al., 2012), though plant roots may also increase expression of extracellular enzymes to improve their antagonistic activity against pathogens (Bolton, 2009; Doornbos et al., 2012). The fungal rather than bacterial community composition was significantly and positively correlated with changes in β-D-cellobiosidase and β-glucosidase associated with root rot disease, suggesting an important role of soil fungi in affecting hydrolases activity. Soil fungal communities represent a major part of the microbial population and predominant decomposers of soil organic compounds (Frey et al., 2014). Soil fungal communities play an important role in regulating soil enzyme activity through synthesizing extracellular enzymes to degrade organic matter (Saiya-Cork et al., 2002). It is likely that the potential leakage of organic root constituents in root rot directly stimulates such hydrolase activities through activated soil fungi. Alternatively, the higher enzymatic potential for hydrolyzing organic matter may be related to higher microbial nutrient demand (Sinsabaugh et al., 2008). The lower SOC content in the diseased soil may in turn stimulate the microorganisms especially the fungi to improve their metabolic function and enzyme activities to degrade both labile and recalcitrant organic matters from plant roots and root-zone soils for survival. Nevertheless, our findings suggest that prolonged root rot infestation has a potential effect on soil enzyme activities through regulation of the fungal community and activity, especially regarding hydrolases involved in C decomposition.

5. Conclusions

Root-rot disease leads to decreases in growth and vitality of *T. grandis*, SOC content and bacterial and fungal abundance. It also changes fungal community composition and functioning towards higher metabolic potential and enzyme activities for C metabolism. These changes induced by root-rot disease may potentially stimulate soil organic matter decomposition.

Acknowledgements

The study was financially supported by National Natural Science Foundation of China under grant number 31570616. We thank the anonymous reviewers for their very valuable comments in improving both the language and scientific quality of the manuscript.

Appendix A. Supplementary material

Supplementary data to this article can be found online at https://doi.org/10.1016/j.foreco.2018.10.028.

References

Bailey, K.L., Lazarovits, G., 2003. Suppressing soil-borne diseases with residue management and organic amendments. Soil Till. Res. 72, 169–180.
Bakker, M.G., Glover, J.D., Mai, J.G., Kinkel, L.L., 2010. Plant community effects on the diversity and pathogen suppressive activity of soil streptomycetes. Appl. Soil Ecol. 46, 35–42.
Bell, C.W., Fricks, B.E., Rocca, J.D., Steinweg, J.M., McMahon, S.K., Wallenstein, M.D., 2013. High-throughput fluorometric measurement of potential soil extracellular enzyme activities. Jove-J. Vis. Exp. 50961.
Benny, G.L., Blackwell, M., 2004. Lobosporangium, a new name for *Echinosporangium Malloch*, and Gamsiella, a new genus for *Mortierella multidivaricata*. Mycologia 96, 143–149.
Bolton, M.D., 2009. Primary metabolism and plant defense—fuel for the fire. Mol. Plant Microbe. In. 22, 487–497.
Bradford, M.M., 1976. A rapid and sensitive method for the quantitation of microgram quantities of protein utilizing the principle of protein-dye binding. Anal. Biochem. 72, 248–254.
Brockett, B.F.T., Prescott, C.E., Grayston, S.J., 2012. Soil moisture is the major factor influencing microbial community structure and enzyme activities across seven biogeoclimatic zones in western Canada. Soil Biol. Biochem. 44, 9–20.
Brussaard, L., Ruiter, P.C.D., Brown, G.G., 2007. Soil biodiversity for agricultural sustainability. Agric. Ecosyst. Environ. 121, 233–244.
Burton, J., Chen, C., Xu, Z., Ghadiri, H., 2010. Soil microbial biomass, activity and community composition in adjacent native and plantation forests of subtropical Australia. J. Soils Sediment. 10, 1267–1277.
Campos, S.B., Lisboa, B.B., Camargo, F.A.O., Bayer, C., Sczyrba, A., Dirksen, P., Albersmeier, A., Kalinowski, J., Beneduzi, A., Costa, P.B., Passaglia, L.M.P., Vargas, L.K., Wendisch, V.F., 2016. Soil suppressiveness and its relations with the microbial community in a Brazilian subtropical agroecosystem under different management systems. Soil Biol. Biochem. 96, 191–197.
Caporaso, J.G., Kuczynski, J., Stombaugh, J., Bittinger, K., Bushman, F.D., Costello, E.K., Fierer, N., Pena, A.G., Goodrich, J.K., Gordon, J.I., 2010. QIIME allows analysis of high-throughput community sequencing data. Nat. Methods 7, 335–336.
Chapon, A., Guillerm, A.Y., Delalande, L., Lebreton, L., Sarniguet, A., 2002. Dominant colonisation of wheat roots by *Pseudomonas fluorescens* Pf29A and selection of the indigenous microflora in the presence of the take-all fungus. Eur. J. Plant Pathol. 108, 449–459.
Chen, J., Sun, X., Li, L., Liu, X., Zhang, B., Zheng, J., Pan, G., 2016. Change in active microbial community structure, abundance and carbon cycling in an acid rice paddy soil with the addition of biochar. Eur. J. Soil Sci. 67, 857–867.
Chen, J., Li, S., Liang, C., Xu, Q., Li, Y., Qin, H., Fuhrmann, J.J., 2017. Response of microbial community structure and function to short-term biochar amendment in an intensively managed bamboo (*phyllostachys praecox*) plantation soil: Effect of particle size and addition rate. Sci. Total Environ. 574, 24–33.
Chen, J., Sun, X., Zheng, J., Zhang, X., Liu, X., Bian, R., Li, L., Cheng, K., Zheng, J., Pan, G., 2018. Biochar amendment changes temperature sensitivity of soil respiration and composition of microbial communities 3 years after incorporation in an organic carbon-poor dry cropland soil. Biol. Fert. Soils 54, 175–188.
Choi, K.H., Dobbs, F.C., 1999. Comparison of two kinds of Biolog microplates (GN and ECO) in their ability to distinguish among aquatic microbial communities. J. Microbiol. Meth. 36, 203–213.
Clarke, K.R., 1993. Non-parametric multivariate analyses of changes in community structure. Austral. Ecol. 18, 117–143.
Clarke, K.R., Warwick, R.M., 2001. A further biodiversity index applicable to species lists: variation in taxonomic distinctness. Marine Ecol. Prog. Ser. 216, 265–278.
Creelman, R.A., Mullet, J.E., 1997. Biosynthesis and action of jasmonates in plants. Annu. Rev. Plant Biol. 48, 355–381.
Davies, T.J., Pedersen, A.B., 2008. Phylogeny and geography predict pathogen community similarity in wild primates and humans. Proc. R. Soc. B 275, 1695–1701.
Dennis, P.G., Miller, A.J., Hirsch, P.R., 2010. Are root exudates more important than other sources of rhizodeposits in structuring rhizosphere bacterial communities? FEMS Microbiol. Ecol. 72, 313–327.
Dick, W.A., Thavamani, B., Conley, S., Blaisdell, R., Sengupta, A., 2013. Prediction of β-glucosidase and β-glucosaminidase activities, soil organic C, and amino sugar N in a diverse population of soils using near infrared reflectance spectroscopy. Soil Biol. Biochem. 56, 99–104.
Donegan, K.K., Schaller, D.L., Stone, J.K., Ganio, L.M., Reed, G., Hamm, P.B., Seidler, R.J., 1996. Microbial populations, fungal species diversity and plant pathogen levels in field plots of potato plants expressing the *Bacillus thuringiensis* var. tenebrionis endotoxin. Transgenic Res. 5, 25–35.
Doornbos, R.F. van, Loon, L.C., Bakker, P.A., 2012. Impact of root exudates and plant defense signaling on bacterial communities in the rhizosphere. A review. Agron. Sustain Dev. 32, 227–243.
Durner, J., Shah, J., Klessig, D.F., 1997. Salicylic acid and disease resistance in plants. Trends Plant Sci. 2, 266–274.
Edgar, R.C., 2013. UPARSE: highly accurate OTU sequences from microbial amplicon reads. Nat. Methods 10, 996–998.
Edgar, R.C., Haas, B.J., Clemente, J.C., Quince, C., Knight, R., 2011. UCHIME improves sensitivity and speed of chimera detection. Bioinformatics 27, 2194–2200.
Fierer, N., Jackson, J.A., Vilgalys, R., Jackson, R.B., 2005. Assessment of soil microbial community structure by use of taxon-specific quantitative PCR assays. Appl. Environ. Microb. 71, 4117–4120.
Fierer, N., Jackson, R.B., 2006. The diversity and biogeography of soil bacterial communities. P. Natl. Acad. SCI. USA 103, 626–631.
Frey, S.D., Ollinger, S., Nadelhoffer, K., Bowden, R., Brzostek, E., Burton, A., Caldwell, B.A., Crow, S., Goodale, C.L., Grandy, A.S., Finzi, A., Kramer, M.G., Lajtha, K., LeMoine, J., Martin, M., McDowell, W.H., Minocha, R., Sadowsky, J.J., Templer, P.H., Wickings, K., 2014. Chronic nitrogen additions suppress decomposition and sequester soil carbon in temperate forests. Biogeochemistry 121, 305–316.
Fu, J., Huang, B., 2001. Involvement of antioxidants and lipid peroxidation in the adaptation of two cool-season grasses to localized drought stress. Environ. Exp. Bot. 45, 105–114.
Gaitnieks, T., Klavina, D., Muiznieks, I., Pennanen, T., Velmala, S., Vasaitis, R., Menkis, A., 2016. Impact of *Heterobasidion* root-rot on fine root morphology and associated fungi in *Picea abies* stands on peat soils. Mycorrhiza 26, 465–473.
Garbeva, P., Veen, J.A., Elsas, J.D., 2004. Microbial diversity in soil: Selection of microbial populations by plant and soil type and implications for disease suppressiveness. Annu. Revi. Phytopathol. 42, 243–270.
Girvan, M.S., Bullimore, J., Pretty, J.N., Osborn, A.M., Ball, A.S., 2003. Soil type is the primary determinant of the composition of the total and active bacterial communities in arable soils. Appl. Environ Microbiol. 69, 1800–1809.
Gordon, T.R., 2017. *Fusarium oxysporum* and the *Fusarium* Wilt Syndrome. Annu. Revi. Phytopathol. 55, 23–39.

Griffiths, B.S., Ritz, K., Wheatley, R., Kuan, H.L., Boag, B., Christensen, S., Ekelund, F., Sorensen, S.J., Muller, S., Bloem, J., 2001. An examination of the biodiversity-ecosystem function relationship in arable soil microbial communities. Soil Biol. Biochem. 33, 1713–1722.
Janvier, C., Villeneuve, F., Alabouvette, C., Edel-Hermann, V., Mateille, T., Steinberg, C., 2007. Soil health through soil disease suppression: Which strategy from descriptors to indicators? Soil Biol. Biochem. 39, 1–23.
Kang, N., Tang, Z.X., 1995. Studies on the taxonomy of genus *Torreya*. Bull. Botanical Res. 15, 349–362.
Kennedy, A.C., 1999. Bacterial diversity in agroecosystems. Agri. Ecosyst. Environ. 74, 65–76.
Kyselkova, M., Kopecky, J., Frapolli, M., Defago, G., Sagova-Mareckova, M., Grundmann, G.L., Moenne-Loccoz, Y., 2009. Comparison of rhizobacterial community composition in soil suppressive or conducive to tobacco black root rot disease. ISME J. 3, 1127–1138.
Li, T., Hu, Y., Du, X., Tang, H., Shen, C., Wu, J., 2014. Salicylic acid alleviates the adverse effects of salt stress in *Torreya grandis* cv. merrillii seedlings by activating photosynthesis and enhancing antioxidant systems. PLoS One 9.
Harmut, A., Lichtenthaler, K., 1987. Chlorophylls and carotenoids - pigments of photosynthetic biomembranes. Methods Enzymol. 148, 350–382.
Lu, R.K., 2000. Methods of soil and agro-chemical analysis. China Agricultural Science and Technology Press, Beijing (in Chinese).
Marschner, P., Kandeler, E., Marschner, B., 2003. Structure and function of the soil microbial community in a long-term fertilizer experiment. Soil Biol. Biochem. 35, 453–461.
Nannipieri, P., Ascher, J., Ceccherini, M.T., Landi, L., Pietramellara, G., Renella, G., 2003. Microbial diversity and soil functions. Eur. J. Soil Sci. 54, 655–670.
Nannipieri, P., Giagnoni, L., Renella, G., Puglisi, E., Ceccanti, B., Masciandaro, G., Fornasier, F., Moscatelli, M.C., Marinari, S., 2012. Soil enzymology: classical and molecular approaches. Biol. Fert. Soils 48, 743–762.
Nayyar, H., 2003. Accumulation of osmolytes and osmotic adjustment in water-stressed wheat (*Triticum aestivum*) and maize (Zeamays) as affected by calcium and its antagonists. Environ. Exp. Bot. 50, 253–264.
Olander, L.P., Vitousek, P.M., 2000. Regulation of soil phosphatase and chitinase activityby N and P availability. Biogeochemistry 49, 175–191.
Qian, Y., Yi, L., Zhang, C., Yu, S., Shen, L., Peng, D., Zheng, C., 2013. Biomass and carbon storage of public service forests in the central area of Zhejiang Province. Sci. Silvae. Sin. 49, 17–23 (in Chinese).
Qin, H., Wang, H., Strong, P.J., Li, Y., Xu, Q., Wu, Q., 2014. Rapid soil fungal community response to intensive management in a bamboo forest developed from rice paddies. Soil Biol. Biochem. 68, 177–184.
Rousk, J., Baath, E., Brookes, P.C., Lauber, C.L., Lozupone, C., Caporaso, J.G., Knight, R., Fierer, N., 2010. Soil bacterial and fungal communities across a pH gradient in an arable soil. ISME J. 4, 1340–1351.
Ruotsalainen, A.L., Eskelinen, A., 2011. Root fungal symbionts interact with mammalian herbivory, soil nutrient availability and specific habitat conditions. Oecologia 166, 807–817.
Saiya-Cork, K.R., Sinsabaugh, R.L., Zak, D.R., 2002. The effects of long term nitrogen deposition on extracellular enzyme activity in an Acer saccharum forest soil. Soil Biol. Biochem. 34, 1309–1315.
Shishido, M., Sakamoto, K., Yokoyama, H., Momma, N., Miyashita, S.-I., 2008. Changes in microbial communities in an apple orchard and its adjacent bush soil in response to season, land-use, and violet root rot infestation. Soil Biol. Biochem. 40, 1460–1473.
Sinsabaugh, R.L., Lauber, C.L., Weintraub, M.N., Ahmed, B., Allison, S.D., Crenshaw, C., Contosta, A.R., Cusack, D., Frey, S., Gallo, M.E., Gartner, T.B., Hobbie, S.E., Holland, K., Keeler, B.L., Powers, J.S., Stursova, M., Takacs-Vesbach, C., Waldrop, M.P., Wallenstein, M.D., Zak, D.R., Zeglin, L.H., 2008. Stoichiometry of soil enzyme activity at global scale. Ecol. Lett. 11, 1252–1264.
Soil Science Society of China, 1999. Soil Physical and Chemical Analysis. Agricultural Science and Technology, Beijing, pp. 146–226 (in Chinese).
Sun, C., Yang, H., 2013. Control of *Helicobasidium compacum* of Torreya grandis 'Merrillii'. J. Zhejiang For. Sci. & Tech. 23, 43–44.
Thiet, R.K., Frey, S.D., Six, J., 2006. Do growth yield efficiencies differ between soil microbial communities differing in fungal:bacterial ratios? Reality check and methodological issues. Soil Biol. Biochem. 38, 837–844.
Tilman, D., Reich, P.B., Knops, J.M., 2006. Biodiversity and ecosystem stability in a decade-long grassland experiment. Nature 441, 629.
Wagg, C., Bender, S.F., Widmer, F., van der Heijden, M.G., 2014. Soil biodiversity and soil community composition determine ecosystem multifunctionality. Proc. Natl. Acad. Sci. USA 111, 5266–5270.
Wang, Y., Lu, D., 2017. Mapping *Torreya grandis* spatial distribution using high spatial resolution satellite imagery with the expert rules-based approach. Remote Sens. 9, 564.
Wei, Z., Yang, T., Friman, V.-P., Xu, Y., Shen, Q., Jousset, A., 2015. Trophic network architecture of root-associated bacterial communities determines pathogen invasion and plant health. Nat. Commun. 6, 8413.
Wittmann, C., Kähkönen, M., Ilvesniemi, H., Kurola, J., Salkinoja-Salonen, M., 2004. Areal activities and stratification of hydrolytic enzymes involved in the biochemical cycles of carbon, nitrogen, sulphur and phosphorus in podsolized boreal forest soils. Soil Biol. Biochem. 36, 425–433.
Wu, Z., Hao, Z., Zeng, Y., Guo, L., Huang, L., Chen, B., 2015. Molecular characterization of microbial communities in the rhizosphere soils and roots of diseased and healthy *Panax notoginseng*. Anton. Leeuw. Int. J. G. 108, 1059–1074.
Wu, Z., Hao, Z., Sun, Y., Guo, L., Huang, L., Zeng, Y., Wang, Y., Yang, L., Chen, B., 2016. Comparison on the structure and function of the rhizosphere microbial community between healthy and root-rot *Panax notoginseng*. Appl. Soil Ecol. 107, 99–107.
Xu, L., Ravnskov, S., Larsen, J., Nilsson, R.H., Nicolaisen, M., 2012. Soil fungal community structure along a soil health gradient in pea fields examined using deep amplicon sequencing. Soil Biol. Biochem. 46, 26–32.
Yang, C., Crowley, D.E., Menge, J.A., 2001. 16S rDNA fingerprinting of rhizosphere bacterial communities associated with healthy and Phytophthora infected avocado roots. FEMS Microbiol. Ecol. 35, 129–136.
Zhang, C.Q., Zhang, S.Y., Chen, X.L., Qi, Q.Q., Lou, H.Z., 2016. First report of *fusarium crown* and root rot on *torreya grandis* caused by *fusarium oxysporum* species complex in China. Plant Dis. 100, 1500.
Zhang, R., Zhang, Y., Song, L., Song, X., Hänninen, H., Wu, J., 2017. Biochar enhances nut quality of *Torreya grandis* and soil fertility under simulated nitrogen deposition. For. Ecol. Manage. 391, 321–329.
Zhang, R., Zhao, Y., Lin, J., Hu, Y., Hänninen, H., Wu, J., 2019. Biochar application alleviates unbalanced nutrient uptake caused by N deposition in *Torreya grandis* trees and seedlings. For. Ecol. Manage. 432, 319–326.